

26. Z. Stein, M. Susser, G. Saenger, F. Marolla, *Famine and Human Development: The Dutch Hungry Winter of 1944–1945* (Oxford Univ. Press, New York, 1975).
27. Independent Commission on International Humanitarian Issues, *Famine: A Man-made Disaster?* (Vintage, New York, 1985).
28. P. Gill, *A Year in the Death of Africa* (Paladin, London, 1986).
29. Oxfam Public Affairs Unit, *Lessons to be Learned; Drought and Famine in Ethiopia* (Oxfam, Oxford, 1984).
30. B. Currey and G. Hugo, in (4) p. 4.
31. J. Sarma, *Contingency Planning for Famines and Other Acute Food Shortages: A Brief Review* (International Food Policy Research Institute, Washington, DC, 1983), append. 2.
32. Ministry of Agriculture and Irrigation, Government of India, Department of Agriculture and Cooperation, *Drought Management 1979* (Offset Press, Directorate of Extension, Ministry of Agriculture and Irrigation, New Delhi, 1979).
33. A. Berg, *Famine Contained: Notes and Lessons from the Bihar Experience* (Brookings Institution, Washington, DC, 1971), report 211.
34. V. Ramalingaswami *et al.*, in (2), p. 94–110.
35. V. Subramanian, *Parched Earth: The Maharashtra Drought 1970–73* (Orient Longman, Bombay, 1975).
36. E. Clay and E. Everitt, Eds., *Food Aid Emergencies: A Report on the Third IDS Food Aid Seminar* (Institute of Development Studies, Univ. of Sussex, Brighton, 1985), disc. pap. 206.
37. R. Montgomery, *Disasters* 9, 163 (1985).
38. J. Holm and R. Morgan, *J. Mod. Afr. Stud.* 23, 463 (1985).
39. M. Hinchley, Ed., *Proceedings of the Symposium on Drought in Botswana* (Botswana Society and Clark Univ. Press, Gaborone, Botswana, 1979).
40. R. Morgan, *Disasters* 9, 44 (1985).
41. H. Ezekiel, "A rural employment guarantee as an early warning system" (International Food Policy Research Institute, Washington, DC, in press).
42. H. Leibenstein, in *Famine*, K. Cahill, Ed. (Orbis, New York, 1982).
43. J. Mellor and B. Johnston, *J. Econ. Lit.* 22, 531 (1984).
44. J. Mellor, in *Development Strategies Reconsidered*, J. P. Lewis and V. Kallab, Eds. (Transaction Books for the Overseas Development Council, New Brunswick, NJ, 1986).
45. D. Jha, "Issues in agricultural technology—Senegal" (International Food Policy Research Institute, Washington, DC), unpublished manuscript.
46. J. Mellor, *The New Economics of Growth: A Strategy for India and the Developing World* (Cornell Univ. Press, Ithaca, NY, 1976), p. 80, table VI-1.
47. Food and Agriculture Organizations, *Food-Crops and Shortages* (various issues, Rome, 1983–1985).
48. Foreign Affairs Committee, *Famine in Africa* (House of Commons, Her Majesty's Stationery Office, London, 1985).
49. S. Kumar, in *Accelerating Food Production in Sub-Saharan Africa*, J. Mellor, C. Delgado, M. Blackie, Eds. (Johns Hopkins Univ. Press, Baltimore, 1987).
50. The World Bank, *World Development Report 1986* (Oxford Univ. Press, New York, 1986), table 27.
51. L. Paulino, *Food in the Third World: Past Trends and Projections to 2000* (Res. Rep. 52, International Food Policy Research Institute, Washington, DC, 1986), table 6.
52. F. Sanderson, *Food Policy* 9, 363 (1984).
53. J. Mellor and C. Ranade, "Technological change in a low labor productivity, land surplus economy: The African development problem" (International Food Policy Research Institute, Washington, DC), unpublished manuscript.
54. R. Ahmed and N. Rustagi, "Agricultural marketing and price incentives: A comparative study of African and Asian countries" (International Food Policy Research Institute, Washington, DC, 1985), unpublished manuscript.
55. S. Nicholson, *Mon. Weather Rev.* 111, 1648 (1983), figure 2.
56. G. Mack, *Devel. Coop.* 4 (July–August 1985), pp. 18–21.
57. International Road Federation, *World Road Statistics* (Geneva, 1982).
58. We are greatly indebted to J. S. Sarma, R. Ahmed, and H. Ezekiel, as well as S. Kumar, E. Kennedy, and B. Stone for their valuable input and comments.

Focal Points in Mass Spectrometry

W. N. DELGASS AND R. G. COOKS

Mass spectrometry has advanced with the renaissance of time-of-flight mass analysis, the use of ion traps as analyzers and reactors, the application of tandem mass spectrometers to problems in ionic reaction mechanisms and chemical analysis, and the development of new desorption ionization techniques. These developments have allowed determination of the molecular weight distributions for polymers through the 10,000-dalton range, as well as the molecular weight and partial sequence of biopolymers of similar size. Surfaces can be characterized by use of the mass, energy, and angle distributions of particles ejected by sputtering or by laser-induced desorption. Mass spectrometry has yielded new information on the kinetics of catalytic surface reactions and on the reactivity of metal clusters.

THE APPLICATIONS OF MASS SPECTROMETRY HAVE SPREAD into physical chemistry (bond dissociation energies, ion enthalpies, proton affinities), organic chemistry (structure elucidation, organic ion structure and fragmentation), the biological sciences (drug metabolism, stable isotope tracer work, modifications in biopolymers), the earth sciences (chronology), and environmental science (trace organic analysis). Important contributions have been made to surface and materials sciences in the past, and it is in these areas that we foresee dramatic progress.

In this article we examine a number of selected areas in which mass spectrometry appears particularly vigorous, or poised to become so. Special emphasis is placed on those aspects that impinge on surface science. In each area the treatment is both expository and critical. We restrict attention to particular work, so that each subject is focused sharply, and attention can be devoted to its impact and future direction.

The traditional divisions in science are yielding, and, when divisions give way, new interdisciplinary alliances emerge. The cross-disciplinary areas of science cluster around particular techniques, not least around mass spectrometry, a subject that has great depth and breadth. The growing importance of instrumentation in science has been noted by Abelson, who wrote "instruments shape research, determine what discoveries are made and perhaps even select the types of individuals likely to succeed as scientists" (1, p. 182).

Ion Chemistry

The applications of mass spectrometry require two principal capabilities, the generation of ions with masses indicative of the molecular weight of the analyte and the formation of fragment ions from which molecular structure can be inferred. Although spectral comparison is the principal method used in arriving at structures, the correlation of spectra with structure is based ultimately on an

The authors are at the School of Chemical Engineering and Department of Chemistry, Purdue University, West Lafayette, IN 47907.

understanding of gas-phase ion chemistry. The increasing interest in the use of artificial intelligence and expert systems in mass spectrometry (2) provides additional impetus for understanding ionic fragmentations and gas-phase ion structures. Although this is a mature area, instrumental developments have produced significant recent advances.

Two examples can be cited. (i) A new class of fragmentation processes, termed remote site fragmentations (3), has been discovered. These reactions are driven by vibrational energy in a region of the molecule where electron densities are not affected significantly by the charge site. (ii) Direct elucidation of the structures of the neutral fragments resulting from ionic dissociation is a valuable new tool (4), which can reveal unexpected complexities in purportedly simple fragmentations.

These discoveries in ion chemistry were directly dependent on developments in instrumentation. Specifically, the discovery of remote site fragmentations depended on two techniques, desorption ionization for producing ions from nonvolatile compounds (5) and tandem mass spectrometry (MS-MS) (6) for characterizing the reactions of particular ions. Neutral fragment characterization depends on techniques that allow ionization of fast-moving neutral beams by charge stripping (that is, electron loss upon collision) (7).

Normally, unimolecular dissociations of ions occur in the vicinity of and under the influence of charged or radical sites in the ionized molecule. Remote site dissociations have been discerned through the study of the collision-activated dissociation of ions containing long hydrocarbon chains, R, for example, RCO_2^- , ROHLi^+ , and even phosphatidylserine ions (3, 8). Remote site C-C cleavages are observed in the alkyl chains of these molecules but are attenuated in the vicinity of double bonds. This provides a simple method for recognizing sites of unsaturation.

The following sequence is an example of such an experiment. A Li^+ ion is attached to an unsaturated long-chain alcohol during fast atom bombardment of a mixture of the alcohol and a lithium salt in glycerol. The parent lithiated molecule can be mass-selected and fragmented upon collision with a gaseous target to produce a set of daughter fragment ions, which can then be mass analyzed. Figure 1 reproduces such a daughter (MS-MS) spectrum. It shows that C-C cleavages occur with a characteristic pattern and can be used to determine the site of unsaturation.

An example of results of ion chemistry now emerging from

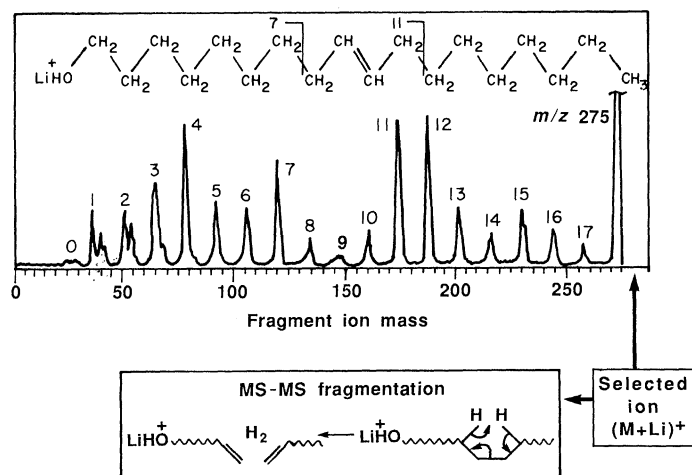


Fig. 1. Remote site fragmentation of a lithiated C_{18} -alkenol generated by FAB. The position of the double bond is determined from the MS-MS spectrum of $(\text{M} + \text{Li})^+$ as shown. Allylic cleavages give abundant C_7 and C_{11} fragments, whereas vinyl cleavages, and especially olefinic cleavages, give a low abundance at mass fragments with 8, 10, and 9 carbons, respectively. [Adapted from (8)]

structural characterization of neutral fragments is the discovery that the neutral fragment arising from dissociation of methyl acetate has the hydroxymethyl (CH_2OH) structure, not the expected methoxy (CH_3O) structure (9). Clearly this reaction cannot occur by the simple bond cleavage usually imagined.

A significant trend in ion chemistry is the growing alliance between those providing ab initio calculations of gas-phase ion structures and the experimentalists (10). Another is the important role of charge-changing collisions (stripping, neutralization, reionization, charge inversion) of high-velocity ion beams, which are essentially vertical Franck-Condon processes, in characterizing ion structure. The high quality of the analytical information obtained by remote site fragmentation suggests a need to produce highly excited ions, whose dissociation behavior should be simpler than that of their low-energy counterparts.

Ion Storage Mass Spectrometers

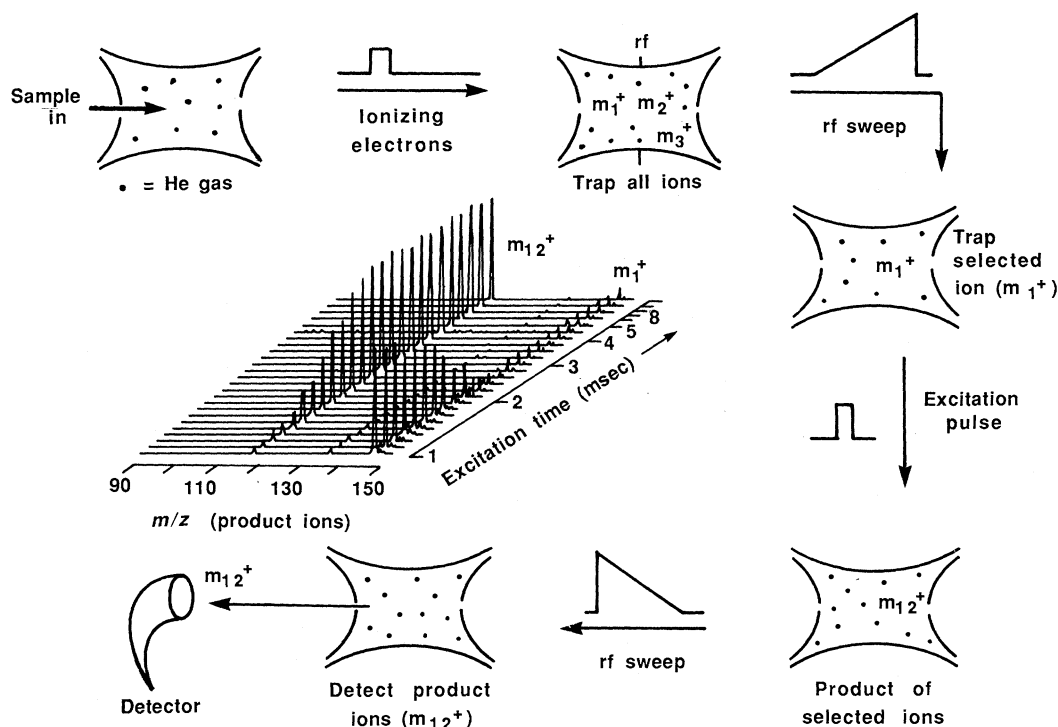
Mass spectrometers that produce beams of ions yield structural information from analysis of collisional processes. A contrasting instrument design allows ions to be trapped either before or in the course of mass analysis. Ion storage mass spectrometers have two specialized features: (i) ions can be accumulated for subsequent experiments, (ii) a time axis can be imposed upon ionic reactions.

Two designs have been explored: ion cyclotron resonance mass spectrometers (11), which use trapping in a magnetic field, and quadrupole ion traps (12), which use electrostatic confinement. Mass analysis can be achieved in various ways with these devices, but two procedures are widely used. In ion cyclotron resonance (ICR), a radio-frequency (rf) excitation pulse is used to excite ions of appropriate cyclotron frequency, thus identifying the mass. The excited ions move in phase and are sensed by the image current induced in the walls of the confinement vessel. Fourier transformation of the time response to an rf "chirp" of frequencies yields a mass spectrum. Fourier transform ICR, or FTMS instruments are being used in a wide range of applications, including the study of organometallic gas-phase ion chemistry and structural studies of biological compounds ionized in situ through the use of secondary ion mass spectrometry (SIMS) or of laser desorption. These applications are facilitated by the high mass resolution and by MS-MS capabilities.

The quadrupole ion trap uses an electric field to exert a force that depends quadratically on the excursion of an ion from the center of the device. Mass analysis can be achieved in various ways, the newest and most promising being mass selective instability (13), a mode in which ions with increasing mass-to-charge (m/z) ratios are ejected sequentially from the trap. As the rf voltage is raised, ions that were stable begin to oscillate and achieve amplitudes that take them beyond the confines of the trap and into a detector.

Two significant developments in such trapping devices have exciting implications. The first addresses the major limitation of the FTMS instrument, that its superb performance is attainable only under ultrahigh vacuum conditions. When ions are produced outside the mass analysis cell, a variety of ionization and sample introduction methods can be used to improve the utility of these instruments. A dual cell design (14) can be used, or, for complete separation of the sample introduction and ionization operations from those of mass analysis, the ICR cell can be coupled through an rf quadrupole ion lens to an external ion source (15). The latter approach has yielded excellent results with compounds such as porcine insulin (molecular weight ~ 5800). Full spectra are obtained routinely from 100-pmol samples. Resolutions of 100,000 can be achieved for organic compounds up to 1700 daltons. This perform-

Fig. 2. Series of daughter spectra showing how dissociation of mass-selected SiEt_4^+ (m_1^+) to give SiEt_3^+ ions (m_{12}^+) is controlled by the time that the excitation pulse is on. The experiment is done in an ion trap with separation in time of ion formation, mass-selection, excitation, and product mass analysis. [Adapted from (18)]



ance is rapidly approaching that available from sector instruments (16). An alternative approach is to use laser-induced desorption (LID) or Cs^+ ion impact to vaporize samples in the cell (17). This approach shows promise in applications to surface science, where ultrahigh vacuum conditions are required.

The electrostatic ion trap has been adapted for MS-MS work as well. Mass-selected ions can be excited and dissociated to produce characteristic daughter ions. The internal energy deposited in the ion is selected through control of collision energy (18). Conditions can be found that maximize the collection of the products of ion-molecule reactions, so that chemical ionization can be induced by various reagents. Figure 2 illustrates MS-MS spectra obtained through use of an ion trap as a function of time. The selected ions, $(\text{C}_2\text{H}_5)_4\text{Si}^+$, are subjected to an excitation pulse at a frequency chosen to selectively excite the molecular ions and cause them to undergo energetic collisions with the helium buffer gas. These collisions result in dissociation to yield an m/z of 115, characteristic of $(\text{C}_2\text{H}_5)_3\text{Si}^+$. Its abundance therefore increases with excitation time. At higher excitation voltages more extensive fragmentation is observed.

Ion traps are relatively inexpensive (the most inexpensive MS-MS instruments available commercially), but they display great versatility. FTMS instruments offer the ultimate in mass resolution at present, and show great promise in the characterization of surfaces and in the study of biological compounds.

Ion-Surface Interactions

The literature of mass spectrometry (19) reveals the importance of experiments in which polyatomic ions dissociate by collision with a gas. The use of collisional excitation is encountered frequently, chiefly for obtaining structural information on selected ions in the MS-MS experiment. These experiments have two disadvantages: (i) the excited ions produced have a broad distribution of internal energies that is difficult to characterize, and (ii) it is difficult to generate the high internal energies that seem to be necessary to dissociate large biological ions (20). Photodissociation (21) rep-

resents one route to solving the first problem, particularly in fundamental studies of ion structure and reactivity. Adaptation of collisional activation in which the collision energy or scattering angle is varied (22) is another. Investigators have begun to address the second issue by utilizing a solid surface in place of a gaseous target.

Collisions of polyatomic ions with solids provide an effective method of exciting, and hence dissociating, these ions (23). Figure 3 shows a plot of the fragmentation behavior as a function of collision energy for mass-selected tetraethylsilane (SiEt_4) molecular ions, which had impacted a gas-covered metal surface. The thermochemistry of some of the fragmentation reactions is known, and a remarkable feature of these data is the large internal energies (~ 15 eV) that can be deposited in SiEt_4^+ at relatively low collision energies.

A range of processes occurs in competition with simple inelastic collisions (Fig. 3). Reactive collisions, in which surface atoms or groups are transferred from molecules adsorbed on the surface to the impacting ion, occur with high specificity for ionic structure. For example, hydrogen atom transfer to ionized acetaldehyde occurs much more readily than to its isomer, ionized ethylene oxide.

The interaction of organic ions with surfaces illustrates one theme of this review, the influence of new instrumental capabilities on the development of science. These techniques promise to develop in three ways: (i) MS-MS instrumentation might be simplified by dispensing with collision gas introduction and control systems; small instruments based on surface dissociation may be used for mixture analysis in field operations. (ii) The high internal energies that can be deposited should assist in obtaining structural information on refractory biological compounds which otherwise resist dissociation. (iii) Reactive collision processes are of potential value in characterizing organic functional groups on surfaces.

Time-of-Flight Analysis

A recent renaissance in this simple method of mass analysis promises to increase its use greatly. Time-of-flight (TOF) methods

convert flight time to m/z ratios, based on the different velocities of ions which vary in mass but have the same kinetic energy. Ion production is pulsed to avoid overlapping signals. All ions in a pulse can be detected and measured; this gives the technique a great advantage in the signal-to-noise (S/N) ratio over methods that disperse ions in space and do not use position-sensitive detectors. In practice, however, resolution of all the ions in a single pulse is not yet possible. Therefore, multiple pulses are needed to record a full mass spectrum, leading to a low-collection duty cycle, as well as a low duty cycle for operation with the source on.

Two major advances in the TOF method are occurring. First, the low duty cycle inherent in the pulsed mode of operation may be eliminated by time array detection (24) or by the use of Fourier transformation (25). The latter experiment uses quasi-continuous ion production and a gating scheme to modulate the allowed flight time. Data are recorded as a function of the frequency of modulation. Fourier transformation of the interferogram recorded in the frequency domain gives the desired time (mass) domain spectrum.

Two new approaches address the issue of resolution, long a weakness of TOF and not subject to improvement by FT methods. One is to use focusing to compensate for the consequences of a spread in initial position (δx), energy (δE), and direction ($\delta \theta$) of the ions before analysis. The other is to minimize the spread in these quantities by careful control of the ionization process.

Time-focusing for different initial positions of ion formation along the mass spectrometer axis is accomplished routinely by using

a two-stage accelerating field. Time-focusing for different initial kinetic energies (velocities) can be achieved by electrostatic reflection (26), or through use of more complex electric or magnetic fields, which are capable of angular focusing (27). In an experiment such as the SIMS analysis of high molecular weight polymers, there are two aspects to time-focusing. First, the incident bombarding ions must interact with the sample in as narrow a time window as possible. Although short pulses are achieved readily for laser desorption, that technique is not nearly as successful as SIMS for ionizing polymers. This requires time-focusing of the primary ion beam to 1 nsec. Second, the secondary ions must be time-focused (if they have the same mass) or time-dispersed (if they do not). A novel procedure for achieving time-focusing of beams having a range of angular and kinetic energies uses toroidal electrostatic analysis (28). The strategy is a more complicated version of that used in conventional double-focusing sector mass spectrometers, which focus ions of the same mass (but different initial directions and velocities) to a single point.

An alternative to focusing is minimization of δx , δE , and $\delta \theta$ during ionization. This has been achieved with pulsed multiphoton ionization of a sample prepared as a molecular beam (29), or alternatively produced by laser desorption from a suitable surface (30). Similar resolutions ($\sim 10^4$) have been obtained in experiments by Benninghoven and his colleagues (31), using time-focusing, and by Reilly and his colleagues (29, 30) by control of the ionization conditions. In these latter experiments the pulse width of the laser (1 to 5 nsec) is the primary factor limiting resolution.

Characterization of Biological Compounds

The need to extend the mass range of mass spectrometers for biological compounds has helped drive recent instrumental developments. Although a relatively low mass range (<4000 daltons), when combined with enzymatic degradation, may suffice for peptide sequencing, other problems might be solved best with the use of mass spectrometers capable of reaching much higher masses. This section deals principally with such instruments.

Three developments are in progress to access high molecular weights. These use different types of mass analyzers and bring contrasting philosophies to the problem. One, FTMS, has been discussed.

Another approach is to build a simple "molecular weight machine," which gives mass range preference over resolution and all other parameters. A commercial embodiment of this approach uses californium fission fragments (32) as energetic particles for desorption ionization and TOF for mass analysis. The high mass range (at least 25 kD for organic molecular ions, above 60 kD for oligomeric ions) and high mass accuracy (± 20 daltons at 25,000 daltons) are coupled appropriately with the californium ionization method, which may be unique (33) for ionizing biological molecules in the mass range of tens of thousands of daltons. Sample sizes required for a full spectrum are in the low nanomole range, although the low detection limits (less than 10^{-16} g) being reported currently for SIMS analysis of precharged compounds after suitable sample preparation (34) imply that this requirement can be reduced. On the basis of the previous discussion of TOF, considerable improvement in the present modest mass resolution could be made, but at a cost in terms of spectrometer complexity. A new experiment (35), in which adsorbed peptides are examined by mass spectrometry, modified chemically in situ, and then reexamined, promises additional structural information in the californium TOF experiment.

In contrast to this simple TOF instrument, the more complex four-sector tandem mass spectrometers (36) attempt to provide both

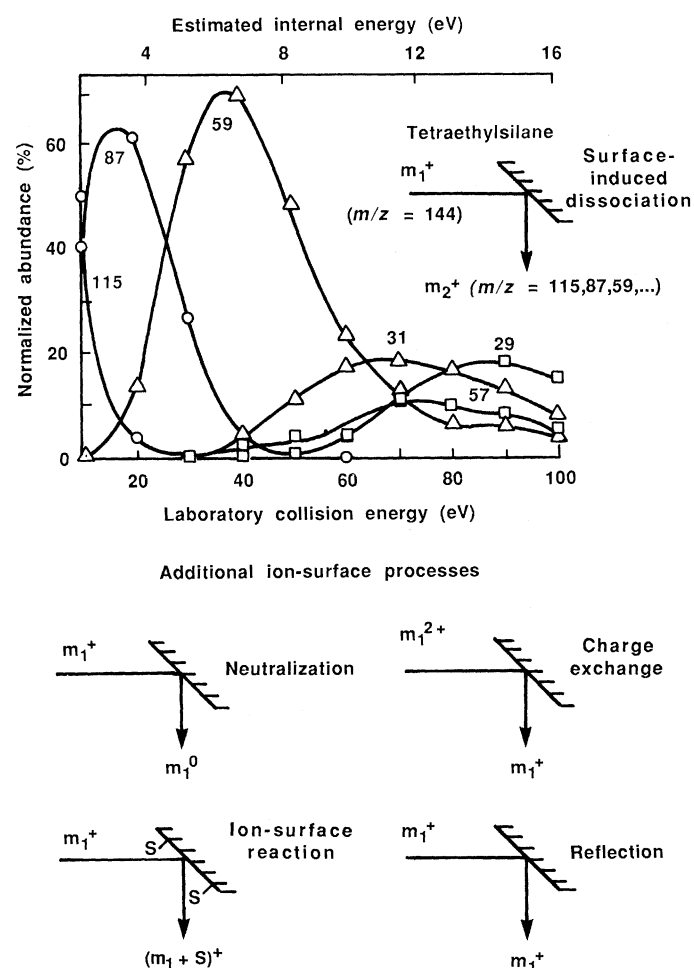


Fig. 3. Energy dependence of dissociation of SiEt_4^+ on collision with a solid surface. Internal energy deposited in the projectile tracks the collision energy. Other processes besides surface-induced dissociation occur as illustrated, including ion-surface reactions with adsorbed species (S) (71).

molecular weight and detailed structural information on biological samples. Fast atom bombardment (FAB) ionization has achieved a molecular weight range of approximately 12,000 daltons for organic compounds. The measurement accuracy of mass is good (much better than unit mass), while the sample size requirements are similar to those for plasma desorption with californium.

Impressive results have been obtained with this type of instrument (37), particularly in the sequencing of peptides of several thousand daltons present in mixtures, with the use of their MS-MS (daughter) spectra. Fragment mass assignments are accurate to the nearest mass unit, the relatively simple spectra being rich in sequence data for selected peptides, even when these are present in mixtures in amounts of just a few nanomoles. The problem of maximizing the efficiency of dissociation of very large (20, 37) biomolecules has been brought into sharp focus by the early results obtained with these instruments. Newer MS-MS scan modes (38), which use more than one fragmentation reaction in sequence, allow cross-checking of ion structures through selective fragmentation processes. For example, one can seek all precursors of a particular ion specified both by its m/z ratio and independently by a characteristic fragmentation reaction.

Other recent developments in ionization methodology also affect the characterization of biological compounds. The matrices from which molecules are ionized in the other desorption ionization techniques are under scrutiny, and improved performance with solid matrices has been noted in SIMS (39) and FAB (40). Californium fission fragment ionization, performed on samples present in a glutathione matrix or supported on nitrocellulose, yields improved S/N ratios and longer-lived and more abundant analyte ions (41). These effects may be related to the role of the matrix in lowering the binding energy of the sample to the substrate, as well as to the decrease in the internal energy of the desorbing ions by solvent shedding.

The mechanism of desorption ionization is still not well understood. One encouraging development is the formulation of a theoretical basis, using Rice-Ramsperger-Kassel-Marcus (RRKM) kinetic formalism, for treating the system after conversion of energy from the form in which it was initially supplied to vibrational energy (42).

Powerful and valuable as the desorption ionization methods have been in biochemistry (43), they have clear disadvantages: (i) samples are introduced in a relatively slow, batchwise fashion through a probe, with the result that these techniques cannot be coupled directly to a chromatograph; and (ii) although various liquid matrices and solutions can be used, aqueous solutions have not been amenable to study. Partial solutions to these problems exist, such as the remarkable thermospray method of combining liquid chromatography with mass spectrometry (44) which sidesteps the desorption ionization methods by using an evaporation procedure instead. An alternative development combines an on-line method of sample introduction with a traditional FAB ionization procedure (45). The result is a system that can utilize 80% aqueous solutions and flow rates in the range compatible with microbore liquid chromatography and still give better sensitivity (10^{-13} mol) than standard FAB techniques with optimized (glycerol) solvents (Fig. 4). Even higher mass samples, for example, bovine insulin, 5730 daltons, produce a molecular ion with good S/N ratios for subnanomole samples.

Surface Layers

If mass spectrometry is to give information on the chemistry and structure of the uppermost layer of atoms of the solid and of molecular adlayers, ejection and ionization mechanisms must be

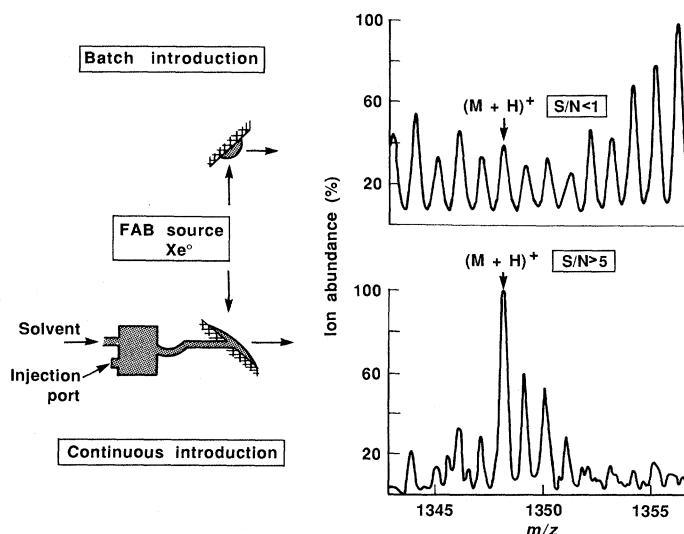


Fig. 4. On-line analysis of a peptide (substance P) in aqueous solution by fast atom bombardment at the 100-fmol level showing improved S/N ratio over conventional FAB. [Adapted from (45)]

understood so that the mass spectrum of the material removed from the surface can be correlated with its original state. We cite two different experiments that meet this criterion. In the first, energy deposited rapidly into the surface by primary ion bombardment (SIMS) (5) or by laser heating (LID) (46–48) causes emission of intact molecular species from the adlayer. In the second, analysis of the angular and energy distributions of ions or neutral species emitted during bombardment with primary ions (49) provides structural information, primarily because emitted particles have high intensity in directions not blocked by surface or adlayer atoms.

In the SIMS versions of these experiments, much of the energy of the primary ion is carried by a collision cascade into the crystal, but some atoms, predominantly those on the surface, can acquire enough energy to overcome cohesion and be ejected from the solid. If the solid is composed of molecules with stronger intramolecular than intermolecular bonding, the tendency to break the weak bonds preferentially will result in intact emission of structurally significant species, including intact molecules (5, 49).

For studies of adsorbates, a standard SIMS apparatus with quadrupole mass detection and ultrahigh vacuum is sufficient. The experiment is shown schematically for Ar^+ primary ions in the lower right quadrant of Fig. 5. Recent SIMS studies of this kind show dehydrogenation of adsorbed ethylene to ethynyl on Pt(111) [indicated by the appearance of CH_3^+ in the SIMS spectrum (50)], the formation of CD by interaction of deuterium with surface carbon on Ru(001) (51), and the synthesis of CH_x with $x = 0$ to 3 by reaction of carbon monoxide with hydrogen on Ni(111) (52). Figure 5d, showing the molecular species formed when isobutene is adsorbed on a dehydrated silica-alumina surface at room temperature, illustrates the use of this technique on nonmetallic surfaces (53). The peaks at 57, 69, and 83 daltons indicate fragments of polyisobutene oligomers that form when isobutene is adsorbed on the dehydrated surface (54). Since the major peak for isobutene is expected at 55 daltons $(\text{M}-\text{H})^+$, the high intensity ratio of peaks at 57 versus 55 daltons suggests, as expected, that oligomers are the majority surface species.

If the quadrupole mass spectrometer (QMS) is replaced by a TOF instrument with high mass capability, intact emission of whole polymer chains during SIMS analysis of polymers can be monitored. Such a measurement (55) for a monolayer film of polydimethylsiloxane on silver is shown in Fig. 5b. Above 500 daltons, fragmentation is reduced and the chain length distribution of the polymer is shown

by the main series of peaks represented by $(nR + CH_3 + Ag)^+$, where R is the repeating unit of the polymer. The largest ion detected corresponds to $n = 128$. These results indicate an important advance. Direct observation of key molecular properties such as chain length distribution should facilitate prediction and ultimately allow control of the mechanical and chemical behavior of polymeric materials.

The structural measurements possible from the energy and angular dependences of secondary particle emission are depicted in Fig. 5, a and c. The secondary particle energy distribution maximizes at a few electron volts, but particles with higher energies desorb earlier in the collision cascade and have sharper angular distributions than those particles at lower energy. These higher energy particles are more representative of the original surface. Pyridine at low coverages is known to π -bond to the surface and lie flat. At high coverages, pyridine σ -bonds to the surface and stands nearly perpendicular to it. The polar angle distributions in Fig. 5c show a sharpening associated with the change in orientation of the pyridine (56). Molecular dynamics calculations (49, 56) show that the sharpening of the distribution is caused by the fact that the vertical pyridine molecules block high polar angle emission.

The combination of energy- and angle-resolved detection of emitted particles with molecular dynamic modeling has yielded an important new means of surface structure analysis. In the newest version of this experiment, neutral particles emitted after a primary ion pulse are ionized by multiphoton resonance ionization (MPRI) and their trajectories are detected on a channel plate detector located above the surface. TOF is used for kinetic energy selection. This approach detects neutral species which are more abundant than ions and less susceptible to yield changes with surface chemistry. Neutral species are modeled directly by molecular dynamics calculations. Ionization occurs selectively only for the species of interest. Results (57) of these measurements on well-defined surfaces are reproduced in Fig. 5a. The lines are experimental polar angle distributions for rhodium emitted at two different energies from Rh(111) with an adsorbed oxygen overlayer which has $p(2 \times 2)$ symmetry. The agreement of molecular dynamics calculations made for oxygen adsorbed in threefold sites, shown as open points, with the experimental data strongly supports assignment of oxygen to that site. Refined calculations can be expected to produce bond distances and

reveal mechanisms of cluster ion formation that are structure-specific (49).

The specificity and efficiency of multiphoton resonance ionization (58) make it an important tool for trace analysis and structural characterization. It can characterize isomeric and isotopic organic compounds, where information taken from the wavelength dependence complements the mass spectrum (59). Impurities in silicon have been detected at the 30 parts-per-billion level in spite of the isobaric overlap of iron and disilicon (60).

The short duration of laser pulses provides a time mark for a variety of TOF experiments. In LID experiments, the short duration and high power density of the pulses combine to produce an intense local heating. LID is a variant of temperature-programmed desorption (TPD). At the fastest heating rates possible in conventional TPD ($\sim 10^2$ K per second), the reaction rates of active surface intermediates are much faster than desorption rates. Thus, only stable products are desorbed, and the reactive surface intermediates must be inferred from the data. At heating rates as high as 10^{11} K per second, however, LID can cause direct desorption of intermediates from the surface.

The instrumentation is shown schematically in Fig. 6. Since each laser pulse completely cleans a small area of the surface, the scanning mirror moves the laser spot to unused areas as the reaction proceeds. Studies of methanol decomposition on Ni(100) demonstrate the power of the method (46). Methanol was adsorbed at 100 K and the sample was heated resistively at 6 K per second. TPD alone would show desorption of hydrogen and carbon monoxide at 325 and 430 K, respectively. The LID curves reveal that the decomposition of methanol begins before the desorption of hydrogen (Fig. 6). Coadsorption of deuterium with methanol produced no deuterium-labeled methanol, which supports the conclusion that the LID signals are indicative of surface concentrations, and not of recombination during desorption. In a second experiment, the laser is pulsed in sequence without moving the spot. The first pulse cleans the surface, and subsequent pulses quantitatively monitor surface diffusion from the perimeter into the sampling area. Recent studies evaluated the coverage dependence of the activation energy and pre-exponential factor for surface diffusion of hydrogen and deuterium on Pt(111) (47). Studies of carbon monoxide desorption from copper based on TOF methods show the velocity distribution to be

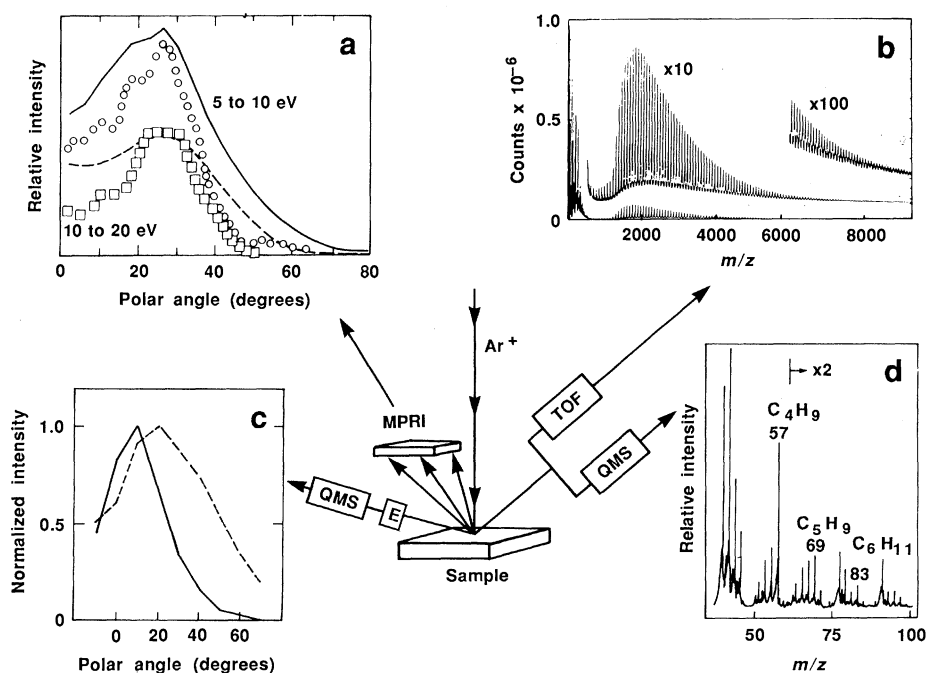


Fig. 5. Schematic diagram of secondary particle emission experiments. (a) Energy- and angle-resolved spectra for rhodium from Rh(111) covered by a $p(2 \times 2)$ oxygen layer. The lines are experimental results obtained by multiphoton resonance ionization. The points are molecular dynamics calculations for oxygen in threefold sites (57). (b) SIMS of polydimethylsiloxane (55). (c) Angular-dependent SIMS spectra for 0.15-langmuir ($1 \text{ langmuir} = 10^{-6} \text{ torr-sec}$) pyridine [dashed line, $(M + H)^+$] and 4.5-langmuir pyridine [solid line, $(M + H)^+$] on Ag(111) (56). The ions are energy-selected (E) before entering the QMS. (d) SIMS of isobutene oligomerized on dehydrated silica-alumina at 300 K (53).

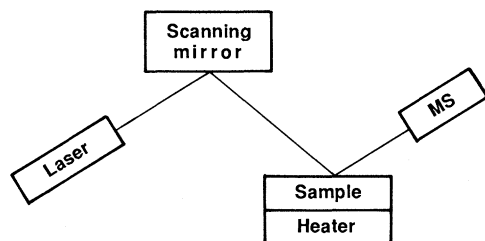
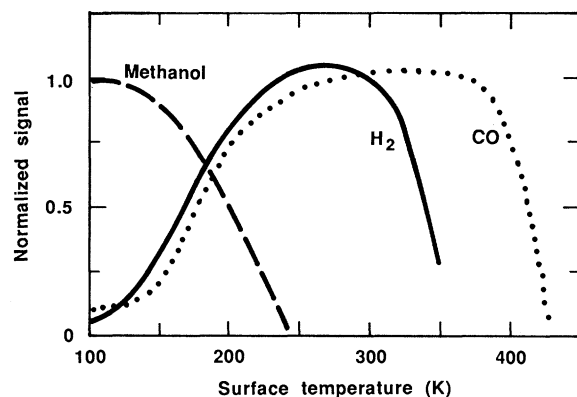


Fig. 6. Schematic for the LID experiment and data for methanol adsorbed on Ni(100) at 100 K and heated at a rate of 6 K per second. [Adapted from (46)]

Boltzmann but, surprisingly, at a lower temperature than that of the surface (48).

High sensitivity and ultrahigh mass resolution can be combined by the use of FTMS for surface analysis. One such instrument (61) used to study small molecules on a stepped platinum surface has a detection limit for carbon monoxide of 5×10^{-6} monolayer and a resolution of 120,000. As Sherman *et al.* pointed out (61), this approach could detect species directly emitted from the surface. This would allow observation of highly reactive fragments that would otherwise be lost to subsequent reactions occurring through collision with the spectrometer walls.

Kinetics of Catalytic Reactions

Although surface analysis is an important element in the understanding of the behavior of solid catalysts, knowledge of a catalytic system is not complete unless the surface chemical properties can be associated with catalytic reaction steps. Traditional steady-state analysis of reactions provides some of the kinetic data needed, but one can obtain additional kinetic information by observing the dynamic response of the system to sudden changes in reactant concentration or isotope identity. The principles of the transient kinetic experiment are well defined. The challenges are in instrumentation, primarily those of creating sharp-edged stimuli and minimizing diffusional and backmixing degradation of the responses as gases pass from the reactor through an inlet to a high-speed detector. Instruments now use quadrupole mass analyzers as detectors and have response times of 0.1 to 10 seconds and data acquisition rates of approximately 50 Hz. Since many catalytic reactions have specific rates of less than one molecule converted per site per second, these instrumental response times are sufficient for a wide variety of kinetic studies.

Transient data can provide several kinds of information. From material balances on the reactor, the capacity of the catalyst surface to adsorb various species can be determined. Relative response times and signal magnitudes corresponding to different isotopically la-

beled species can indicate the slow steps in a reaction sequence. Curve fitting, based on the full time-dependent differential equations, provides a demanding test of the proposed sequence of elementary kinetic steps and produces more reliable kinetic parameters than steady-state analysis, which is based on the asymptotic solution of the equations. Although the overall rates may be relatively slow, adsorption steps can proceed with time constants of microseconds. Since macroscopic mixing on this time scale is virtually impossible at atmospheric pressure, concentration jumps will often produce a spatial as well as a temporal transient in the reactor. Modeling and even qualitative interpretation are greatly simplified when changes due to introduction of isotopically labeled compounds are followed at steady-state reaction conditions. If the kinetic isotope effect and reverse reaction rates are small, the rate is the same at all points in the catalyst bed and only time dependences need be considered.

Applications of these principles have focused recently on hydrocarbon synthesis reactions (62). Kinetically important CH_x species have been identified on iron and nickel. Dynamic responses to ^{13}CO substitution have shown that carbon monoxide dissociation can be rate limiting on platinum but not on nickel. Substitution sequences involving ^{13}CO and deuterium over ruthenium catalysts have shown that carbon is present on the surface in different forms, and that the surface also has a surprisingly high inventory of hydrogen. Figure 7 illustrates isotopic substitution studies of the ethylene epoxidation reaction over silver powder (63). This reaction has been much studied, but questions remain concerning the nature of the active oxygen species (64). Figure 7 summarizes two experiments carried out at 473 K, 171 torr of oxygen, 154 torr of ethylene, and 418 torr of argon. In the first experiment, $^{18}\text{O}_2$ is substituted for normal oxygen during reaction. The argon curve shows the response of gas not adsorbed by the catalyst and serves as a time mark for the pulse. The close overlay of the argon and labeled oxygen curves shows that

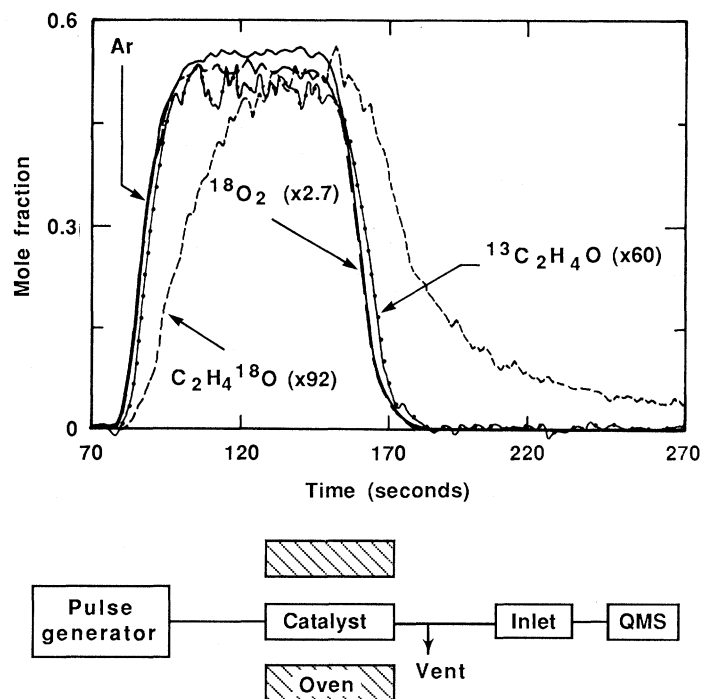


Fig. 7. Schematic for transient kinetic experiment and data (63) for isotopic transient during ethylene epoxidation at 473 K and at pressures in torr of $P_{\text{O}_2}:P_{\text{C}_2\text{H}_4}:P_{\text{Ar}} = 171:154:418$ over a silver powder catalyst. The argon curve indicates the pulse shape and timing. $\text{C}_2\text{H}_4^{18}\text{O}$ is the response to a switch from $\text{C}_2\text{H}_4 + ^{16}\text{O}_2$ to $\text{C}_2\text{H}_4 + ^{18}\text{O}_2$ and back. $^{13}\text{C}_2\text{H}_4\text{O}$ is the response to a switch from $\text{C}_2\text{H}_4 + \text{O}_2$ to $^{13}\text{C}_2\text{H}_4 + \text{O}_2$ and back. The $^{13}\text{C}_2\text{H}_4$ pulse follows the argon trace closely and is not shown.

the surface has little capacity for exchangeable molecular oxygen at reaction conditions. This is consistent with pulsed oxygen adsorption experiments, which show that oxygen uptake is high but completely irreversible at 473 K. The slow response of labeled ethylene oxide to $^{18}\text{O}_2$ substitution shows that ethylene oxide is formed from the large, irreversibly adsorbed pool of surface oxygen, not from a small number of reversibly adsorbed oxygen species that would incorporate the label rapidly. Since the irreversibly adsorbed oxygen is atomic rather than molecular at these temperatures, the results support addition of atomic oxygen as the rate-limiting step in the formation of ethylene oxide under these reaction conditions. Ethylene adsorption is reversible and has less capacity than oxygen. Thus, the fast response of ^{13}C -ethylene oxide to ^{13}C -ethylene, also shown in Fig. 7, is expected and confirms that the slow oxygen-labeled ethylene oxide response is kinetically controlled and not caused by experimental artifacts, such as adsorption on the walls of the apparatus.

In general, since the kinetic analysis described here is related to surface analysis, surface concentration terms appear in the differential equations used to model the kinetic responses. Simultaneous in situ measurement of the responses of the surface concentrations can add new information and further increase the reliability of the resulting models and parameters.

Clusters

A question of long standing in the study of reactivity at surfaces concerns the effect of particle size of the solid entity. The conversion from an atomlike to a cooperative electronic structure is a function of size. Also, the possible changes in structure, bond lengths, and the influence of bonding to the support for small ensembles of atoms suggest that the properties of the particle itself and its ability to adsorb gases and catalyze surface reactions can be a function of size.

The difficulty of preparing well-defined samples has hampered progress in understanding size effects. Recently, it has become possible to study and prepare gas-phase clusters by development of instruments that use laser ablation of a substrate into a pulsed supersonic gas flow to create the clusters. Photoionization followed by TOF allows mass analysis of the cluster distribution (65, 66). Reactivities of the clusters are measured by mixing the entrained cluster flow with the reaction gas and measuring product cluster signals. A notable feature of these experiments is the degree of control exerted on the creation and reaction of the clusters through variable timing sequences (67). Desorption of the cluster material uses a pulsed laser. The expansion (condensation) stage of the helium flow occurs for a set interval (10^{-4} second). Reagents are added with a pulsed valve which has variable delay with respect to the helium pulse, and product sampling by laser ionization occurs after a further period of selected duration. These capabilities allow enormous flexibility in the experiment.

We focus on a few examples of reactions of small naked metal clusters with gas-phase molecules. Although iron atoms are unreactive, iron clusters (67) react with oxygen to form Fe_xO_{2y} and with H_2S to form Fe_xS_y . The reactivity increases rapidly with x and levels off when $x = 6$. Reaction with deuterium shows a more complex behavior. For $x > 23$, deuterium is 1/100 as reactive as oxygen or H_2S . A striking reactivity maximum is seen in the region of Fe_{10} , where a corresponding maximum in the ionization potential exists. A similar maximum in reactivity with deuterium has been seen for cobalt clusters (68).

Perhaps most intriguing among the new results on small clusters are findings on the reactivity of platinum (66). For Pt_2 and larger

clusters, the strong dehydrogenation activity of platinum is apparent. A striking similarity is found between the reaction of platinum clusters with benzene and with normal hexane. The latter shows a high degree of dehydrogenation, and perhaps aromatization, on clusters as small as Pt_2 .

If the detection system can differentiate the behavior of clusters of different size, the distribution of particles produced is not crucial. Narrow size distribution is essential, however, for studies in which only reaction products that are released from the particle surface are analyzed. This goal has been achieved with the multiple expansion cluster source (69). It separates the nucleation and growth steps to produce a narrow age distribution and correspondingly narrow size distribution. Experiments with clusters of just one size are being carried out by FTMS (11, 70). This instrument is particularly valuable in the preparation and study of clusters that carry ligands, because reactions can be studied as a function of such chemical properties of the cluster as the degree of coordinative unsaturation and metal-metal and metal-ligand binding energies.

These new instruments and results establish the chemistry of small ensembles. Although the energetic state of the clusters is not always defined, the size specificity reported indicates that this chemistry is rich. Applications of cluster-size effects in fields such as microelectronics or catalysis will require selected size entities stabilized on or in solids. Gas-phase experiments can simulate the first few neighboring atoms of the solid environment.

REFERENCES AND NOTES

1. P. H. Abelson, *Am. Sci.* **74**, 182 (1986).
2. C. J. Wong, *Anal. Chem.* **56**, 1312A (1985); T. H. Pierce and B. A. Holme, Eds., *Artificial Intelligence Applications in Chemistry* (ACS Symposium Series 306, American Chemical Society, Washington, DC, 1986).
3. N. J. Jensen, K. B. Tomer, M. L. Gross, *Anal. Chem.* **57**, 2018 (1985).
4. P. O. Danis, C. Wesdemiotis, F. W. McLafferty, *J. Am. Chem. Soc.* **105**, 7454 (1983).
5. K. L. Busch and R. G. Cooks, *Science* **218**, 247 (1982); A. L. Burlingame and N. Castagnoli, Jr., Eds., *Mass Spectrometry in Health and Life Sciences* (Elsevier, Amsterdam, 1985).
6. R. G. Cooks, K. L. Busch, G. L. Glish, *Science* **222**, 273 (1983); F. W. McLafferty, Ed., *Tandem Mass Spectrometry* (Wiley, New York, 1983).
7. T. Ast, *Adv. Mass Spectrom.*, in press.
8. J. Adams and M. L. Gross, in preparation.
9. J. K. Terlouw, J. L. Holmes, P. C. Bergers, *Int. J. Mass Spectrom. Ion Process.* **66**, 239 (1985).
10. W. Koch, F. Maquin, D. Stahl, H. Schwartz, *Chimia* **39**, 376 (1985).
11. B. S. Freiser, *Talanta* **32**, 697 (1985); D. H. Russell, *Mass Spectrom. Rev.* **5**, 167 (1986); M. L. Gross and D. L. Rempel, *Science* **226**, 261 (1984).
12. J. F. J. Todd, *Dyn. Mass Spectrom.* **6**, 44 (1981).
13. G. C. Stafford, Jr., P. E. Kelley, J. E. P. Syka, W. E. Reynolds, J. F. J. Todd, *Int. J. Mass Spectrom. Ion Process.* **60**, 85 (1984).
14. I. J. Amster *et al.*, *Anal. Chem.* **58**, 483 (1986).
15. D. F. Hunt, J. Shabanowitz, R. T. McIver, Jr., R. L. Hunter, J. E. P. Syka, *ibid.* **57**, 768 (1985).
16. J. Shabanowitz, D. F. Hunt, D. H. Russell, paper FOB9 presented at the 34th annual conference on Mass Spectrometry and Allied Topics, American Society of Mass Spectrometry (ASMS), Cincinnati, June 1986.
17. I. J. Amster, M. E. Costro, D. H. Russell, R. B. Cody, Jr., F. W. McLafferty, *Anal. Chem.* **58**, 485 (1986).
18. J. N. Louris, J. Brodbelt, R. G. Cooks, J. E. P. Syka, G. C. Stafford, Jr., paper ROC15 presented at the 34th annual conference on Mass Spectrometry and Allied Topics, ASMS, Cincinnati, June 1986.
19. A. L. Burlingame, T. A. Baillie, P. J. Derrick, *Anal. Chem.* **58**, 165R (1986).
20. G. M. Neumann and P. J. Derrick, *Org. Mass Spectrom.* **19**, 165 (1984).
21. F. M. Harris and J. H. Beynon, in *Ions and Light*, vol. 3 of *Gas Phase Ion Chemistry*, M. T. Bowers, Ed. (Wiley, New York, 1984), pp. 100-129.
22. S. A. McLuckey and R. G. Cooks, in *Tandem Mass Spectrometry*, F. W. McLafferty, Ed. (Wiley, New York, 1983), pp. 303-320.
23. M. A. Mabud, M. J. DeKrey, R. G. Cooks, *Int. J. Mass Spectrom. Ion Process.* **67**, 285 (1985).
24. B. Eckenrode *et al.*, in preparation.
25. F. J. Knorr, M. Ajami, D. A. Chatfield, *Anal. Chem.* **58**, 690 (1986).
26. B. A. Mamyurin, V. I. Karataev, D. V. Shmikk, V. A. Zagulin, *Sov. Phys. JETP* **37**, 45 (1973).
27. P. Steffens, E. Niehuis, T. Freise, D. Greifendorff, A. Benninghoven, *J. Vac. Sci. Technol.* **A3**, 1322 (1985).
28. T. Sakurai, T. Matsuo, H. Matsuda, *Int. J. Mass Spectrom. Ion Process.* **63**, 273 (1985).
29. R. B. Opsal, K. G. Owens, J. P. Reilly, *Anal. Chem.* **57**, 1884 (1985); R. Tembreull and D. M. Lubman, *ibid.* **56**, 1962 (1984).
30. M. Yang and J. P. Reilly, paper ROD11 presented at the 34th annual conference on Mass Spectrometry and Allied Topics, ASMS, Cincinnati, June 1986.

31. E. Niehuis, T. Heller, H. Feld, A. Benninghoven, in *Ion Formation from Organic Solids, IFOS [Ions from Organic Solids] III*, A. Benninghoven, Ed. (Springer, Berlin, 1986), pp. 198–203.
32. B. Sundqvist and R. D. Macfarlane, *Mass Spectrom. Rev.* **4**, 421 (1985).
33. B. Sundqvist, A. Hedin, P. Hakansson, M. Salehpour, G. Save, *Nucl. Instrum. Methods Phys. Res.* **B14**, 429 (1986).
34. W. Lange, D. Greifendorf, D. van Leyen, E. Niehuis, A. Benninghoven, in *Ion Formation from Organic Solids, IFOS III*, A. Benninghoven, Ed. (Springer, Berlin, 1986), pp. 67–73.
35. B. T. Chait and F. H. Field, *Biochem. Biophys. Res. Commun.* **134**, 420 (1986).
36. P. J. Todd, D. C. McGilvery, M. A. Baldwin, F. W. McLafferty, in *Tandem Mass Spectrometry*, F. W. McLafferty, Ed. (Wiley, New York, 1983), pp. 271–286.
37. K. Biemann *et al.*, in *Mass Spectrometry in the Analysis of Large Molecules* (Proceedings of Texas Symposium on Mass Spectrometry), C. McNeal, Ed. (Wiley, Sussex, United Kingdom, in press).
38. J. N. Louris, L. G. Wright, R. G. Cooks, A. E. Schoen, *Anal. Chem.* **57**, 2918 (1985).
39. R. J. Colton, M. M. Ross, D. A. Kidwell, *Nucl. Instrum. Methods Phys. Res.* **B13**, 259 (1986).
40. B. Ackerman, J. T. Watson, J. Holland, *Anal. Chem.* **57**, 2656 (1985).
41. M. Alai, P. Demirev, C. Fenselau, R. J. Cotter, *ibid.* **58**, 1303 (1986).
42. B. V. King, A. R. Ziv, S. H. Lin, I. S. T. Tsong, *J. Chem. Phys.* **82**, 3641 (1985).
43. For typical solved problems see R. J. Townsend, D. N. Heller, C. C. Fenselau, and Y. C. Lee [*Biochemistry* **23**, 6389 (1984)] and K. J. Hjver, J. E. Campana, R. J. Cotter, and C. Fenselau [*Biochem. Biophys. Res. Commun.* **130**, 1287 (1985)].
44. C. R. Blakely and M. L. Vestal, *Anal. Chem.* **51**, 750 (1983).
45. R. M. Caprioli, T. Fan, J. S. Cottrell, *ibid.*, in press.
46. R. B. Hall and S. J. Bares, in *Chemistry and Structures at Interfaces*, R. B. Hall and A. B. Elles, Eds. (VCH Publishers, Deerfield Beach, FL, 1985), pp. 83–147; R. B. Hall and A. M. DeSantolo, *Surf. Sci.* **137**, 421 (1984).
47. E. G. Seebauer and L. P. Schmidt, *Chem. Phys. Lett.* **123**, 129 (1986).
48. D. Burgess, Jr., R. Viswanathan, I. Hussla, P. C. Stair, E. Weitz, *J. Phys. Chem.* **79**, 5200 (1983).
49. N. Winograd, *Desorption Mass Spectrometry* (ACS Symposium Series 291, American Chemical Society, Washington, DC, 1985), pp. 83–96; B. J. Garrison, *ibid.*, pp. 43–55.
50. J. R. Creighton and J. M. White, *Surf. Sci.* **129**, 327 (1983).
51. L. L. Lauderback and W. N. Delgass, *J. Catal.*, in press.
52. M. P. Kaminsky, N. Winograd, G. L. Geoffrey, M. A. Vannice, *J. Am. Chem. Soc.* **108**, 1315 (1986).
53. P. J. Schumacher and W. N. Delgass, in preparation.
54. J. B. Peri, in *Proceedings of the Third International Congress on Catalysis* (Amsterdam, 20 to 25 July 1964), W. M. H. Sachtler, G. C. A. Schuit, P. Zweitering, Eds. (North-Holland, Amsterdam, 1965), vol. 2, pp. 1100–1112.
55. I. V. Bletsos, D. M. Hercules, D. van Leyen, A. Benninghoven, *Ion Formation from Organic Solids, IFOS III*, A. Benninghoven, Ed. (Springer, Berlin, 1986), pp. 74–78.
56. D. W. Moon, N. Winograd, B. J. Garrison, *Chem. Phys. Lett.* **114**, 237 (1985).
57. N. Winograd *et al.*, *Surf. Sci.* **176**, L817 (1986).
58. G. S. Hurst, M. G. Payne, S. D. Kramer, J. P. Young, *Rev. Mod. Phys.* **51**, 767 (1979).
59. R. Tembreull, Chung Hang Sin, Ping Li, Ho Ming Pang, D. M. Lubman, *Anal. Chem.* **57**, 1186 (1985); D. M. Lubman, R. Tembreull, Chung Hang Sin, *ibid.*, p. 1084.
60. M. J. Pelhen, C. E. Young, W. F. Calaway, D. M. Gruen, *Nucl. Instrum. Methods Phys. Res.* **B13**, 653 (1986).
61. M. G. Sherman, J. R. Kingsley, J. C. Hemminger, R. T. McIver, Jr., *Anal. Chim. Acta* **178**, 79 (1985); M. G. Sherman, J. R. Kingsley, D. A. Dahlgren, J. C. Hemminger, R. T. McIver, *Surf. Sci.* **148**, L25 (1985).
62. D. Bianchi, L. M. Tau, S. Borcar, C. O. Bennett, *J. Catal.* **84**, 358 (1983); M. Otard *et al.*, *ibid.*, p. 156; P. Winslow and A. T. Bell, *ibid.* **91**, 142 (1985); C.-H. Yang, Y. Soong, P. Biloen, *Chem. Commun.* **1985**, 475 (1985).
63. K. J. Warren and W. N. Delgass, in preparation.
64. C. T. Campbell, *J. Catal.* **99**, 28 (1986); R. B. Grant and R. M. Lambert, *ibid.* **92**, 364 (1985); R. A. van Santen and C. P. M. deGroot, *ibid.* **98**, 530 (1986).
65. T. G. Dietz, M. A. Duncan, D. E. Powers, R. E. Smalley, *J. Chem. Phys.* **74**, 6511 (1981).
66. R. L. White, D. J. Trevor, R. L. Whetten, D. M. Cox, A. Kaldor, *J. Am. Chem. Soc.* **107**, 518 (1985).
67. R. L. Whetten, D. M. Cox, D. J. Trevor, A. Kaldor, *J. Phys. Chem.* **89**, 566 (1985); *Phys. Rev. Lett.* **54**, 1494 (1985).
68. M. E. Geusic, M. D. Morse, R. E. Smalley, *J. Chem. Phys.* **82**, 590 (1985).
69. R. S. Bowles, J. J. Kolstad, J. M. Calo, R. P. Andres, *Surf. Sci.* **106**, 117 (1981); R. S. Bowles, S. B. Park, N. Otsuka, R. P. Andres, *J. Mol. Catal.* **20**, 279 (1983).
70. D. J. Anderson, D. J. A. Freedon, D. H. Russell, *J. Am. Chem. Soc.* **107**, 3762 (1985); R. G. Freas and J. E. Campana, *ibid.*, p. 6202.
71. M. Bier and R. G. Cooks, unpublished results.
72. Our task was facilitated by comments and manuscripts received from K. L. Busch, R. J. Colton, C. E. Costello, R. J. Cotter, B. T. Chait, R. M. Caprioli, R. J. Day, C. C. Fenselau, B. J. Garrison, M. L. Gross, D. M. Gruen, R. B. Hall, G. L. Haller, G. B. Hoflund, A. Kaldor, D. M. Lubman, R. T. McIver, Jr., D. H. Russell, L. D. Schmidt, H. Schwarz, K. Shabanowitz, P. C. Stair, D. J. Trevor, and N. Winograd. This research was supported by the National Science Foundation (CHE 84-08258 and DMR 84-18453) and Amoco Oil Company.

The Biology and Chemistry of Fertilization

PAUL M. WASSARMAN

Fertilization of eggs by sperm, the means by which sexual reproduction takes place in nearly all multicellular organisms, is fundamental to the maintenance of life. In both mammals and nonmammals, the pathway that leads to fusion of an egg with a single sperm consists of many steps that occur in a compulsory order. These steps include species-specific cellular recognition, intracellular and intercellular membrane fusions, and enzyme-catalyzed modifications of cellular investments. In several instances, the molecular mechanisms that underlie these events during mammalian fertilization are beginning to be revealed.

AS A CONSEQUENCE OF ITS FUNDAMENTAL ROLE IN THE life history of most higher organisms, fertilization has been of great interest to scientists for more than a century. Building upon original contributions of E. Van Beneden, O. Hertwig, and H. Fol, made between 1875 and 1880, we are rapidly

expanding our understanding of the biology and chemistry of mammalian fertilization. In recent years this knowledge has influenced both medical and ethical aspects of conception and contraception and undoubtedly will continue to do so (1).

I shall describe here some principal cellular and molecular features of fertilization in mammals, from the initial encounter of sperm and egg to their fusion with one another to form a zygote. Although much of the discussion is drawn from in vitro experiments with mouse gametes, it is likely that the stratagem for fertilization described applies to in vivo fertilization for most mammals, including humans. Throughout the article, fertilization in mice is compared with fertilization in sea urchins, the most extensively studied nonmammalian species. Such comparisons illustrate the large number of cellular and molecular features common to fertilization in these two organisms.

This article is not intended to be comprehensive, but should serve only as an introduction to certain aspects of contemporary mamma-

The author is chairman of the Department of Cell Biology at the Roche Institute of Molecular Biology, Roche Research Center, Nutley, NJ 07110.